11 Saito M, Nishikomori R, Kambe N, *et al*. Disease-associated CIAS1 mutations induce monocyte death, revealing low-level mosaicism in mutation-negative cryopyrin-associated periodic syndrome patients. *Blood* 2008;111:2132–41.
12 Cuisset L, Jeru I, Dumont B, *et al*. French CAPS study group. Mutations in the autoinflammatory cryopyrin-associated periodic syndrome gene: epidemiological study and lessons from eight years of genetic analysis in France. *Ann Rheum Dis* 2011;70:495–9.
13 Arostegui JI, Lopez Saldaña MD, Pascal M, *et al*. A somatic NLRP3 Mutation as a cause of a Sporadic Case of CINCA/NOMID Syndrome. Novel evidences of the role of low-level mosaicism as pathophysiological mechanism underlying Mendelian inherited diseases. *Arthritis Rheum* 2010;62:1158–66.
14 Neven B, Marvillet I, Terrada C, *et al*. Long-term efficacy of the interleukin-1 receptor antagonist anakinra in ten patients with Neonatal-Onset Multisystem Inflammatory Disease/Chronic Infantile Neurologic, Cutaneous, Articular syndrome. *Arthritis Rheum* 2010;62:258–67.
15 Aróstegui JI, Aldea AI, Modesto C, *et al*. Clinical and genetic heterogeneity among Spanish patients with recurrent autoinflammatory syndromes-associated to CIAS1/PYPAF1/NALP3 gene. *Arthritis Rheum* 2004;50:4045–50.
16 Saito M, Fujisawa A, Nishikomori R, *et al*. Somatic mosaicism of CIAS1 in a patient with Chronic Infantile Neurologic, Cutaneous, Articular syndrome. *Arthritis Rheum* 2005;52:3579–85.
17 Rynne M, Maclean C, Bybee A, *et al*. Hearing improvement in a patient with variant Muckle-Wells syndrome in response to interleukin 1 receptor antagonism. *Ann Rheum Dis* 2006;65:533–4.
18 Kagami S, Saeki H, Kuwano Y, *et al*. A probable case of Muckle-Wells syndrome. *J Dermatol* 2006;33:118–21.
19 Aksentijevich I, Putnam CD, Remmers EF, *et al*. The clinical continuum of cryopyrinopathies. Novel CIAS1 Mutations in North American patients and a new cryopyrin model. *Arthritis Rheum* 2007;56:1273–85.
20 Ohnishi H, Teramoto T, Iwata H, *et al*. Characterization of NLRP3 variants in Japanese cryopyrin-associated periodic syndrome patients. *J Clin Immunol* 2012;32:221–9.
21 Wise CA, Bennett LB, Pascual V, *et al*. Localization of a gene for familial recurrent arthritis. *Arthritis Rheum* 2000;43:2041–5.
22 Kanazawa N, Okafuji I, Kambe N, *et al*. Early-onset sarcoidosis and CARD15 mutations with constitutive nuclear factor-kappaB activation: common genetic etiology with Blau syndrome. *Blood* 2005;105:1195–7.
23 Aróstegui JI, Arnal C, Merino R, *et al*. NOD2 gene-associated pediatric granulomatous arthritis: clinical diversity, novel and recurrent mutations, and evidence of clinical improvement with interleukin-1 blockade in a Spanish cohort. *Arthritis Rheum* 2007;56:3805–13.
24 Verma D, Eriksson P, Sahdo B, *et al*. Two adult siblings with atypical cryopyrin-associated periodic syndrome due to a novel M299V mutation in NLRP3. *Arthritis Rheum* 2010;62:2138–43.
25 Murphy G, Daly M, O'Sullivan M, *et al*. An unusual phenotype in Muckle-Wells syndrome associated with NLRP3 E311K. *Rheumatology* 2011;50:419–20.
26 Hawkins PN, Lachmann HJ, Aganna E, *et al*. Spectrum of clinical features in Muckle-Wells syndrome and response to anakinra. *Arthritis Rheum* 2004;50:607–12.
27 Lachmann HJ, Kone-Paut I, Kuemmerle-Deschner JB, *et al*. Use of canakinumab in the cryopyrin-associated periodic syndrome. *N Engl J Med* 2009;360:2416–25.
28 Mirault T, Launay D, Cuisset L, *et al*. Recovery from deafness in a patient with Muckle-Wells syndrome treated with anakinra. *Arthritis Rheum* 2006;54:1697–700.
29 Kuemmerle-Deschner JB, Tyrrell PN, Koetter I, *et al*. Efficacy and safety of anakinra therapy in pediatric and adult patients with the autoinflammatory Muckle-Wells syndrome. *Arthritis Rheum* 2011;63:840–9.
30 Weegerink NJ, Schraders M, Leijendeckers J, *et al*. Audiometric characteristics of a Dutch family with Muckle-Wells syndrome. *Hear Res* 2011;282:243–51.
31 Jiménez-Treviño S, González-Roca E, Ruiz-Ortiz E, *et al*. First report of vertical transmission of a somatic *NLRP3* mutation in cryopyrin-associated periodic syndromes. *Ann Rheum Dis* 2013;72:1109–10.

RESEARCH ARTICLE

AMERICAN JOURNAL OF medical genetics PART A

Narrowing of the Responsible Region for Severe Developmental Delay and Autistic Behaviors in WAGR Syndrome Down to 1.6 Mb Including *PAX6*, *WT1*, and *PRRG4*

Toshiyuki Yamamoto,[1]* Masami Togawa,[2] Shino Shimada,[1,3] Noriko Sangu,[1,4] Keiko Shimojima,[1] and Nobuhiko Okamoto[5]

[1]Tokyo Women's Medical University Institute for Integrated Medical Sciences (TIIMS), Tokyo, Japan

[2]Division of Child Neurology, Faculty of Medicine, Tottori University, Yonago, Japan

[3]Department of Pediatrics, Tokyo Women's Medical University, Tokyo, Japan

[4]Department of Oral and Maxillofacial Surgery, School of Medicine, Tokyo Women's Medical University, Tokyo, Japan

[5]Department of Medical Genetics, Osaka Medical Center and Research Institute for Maternal and Child Health, Izumi, Japan

Manuscript Received: 16 April 2013; Manuscript Accepted: 10 September 2013

Interstitial deletions of the 11p13 region are known to cause WAGR (Wilms tumor, aniridia, genitourinary malformation, and "mental retardation") syndrome, a contiguous gene deletion syndrome due to haploinsufficiencies of the genes in this region, including *WT1* and *PAX6*. Developmental delay and autistic features are major complications of this syndrome. Previously, some genes located in this region have been suggested as responsible for autistic features. In this study, we identified two patients who showed the chromosomal deletions involving 11p13. Patient 1, having an 8.6 Mb deletion of chr11p14.1p12:29,676,434–38,237,948, exhibited a phenotype typical of WAGR syndrome and had severe developmental delay and autistic behaviors. On the other hand, Patient 2 had a larger aberration region in 11p14.1–p12 which was split into two regions, that is, a 2.2-Mb region of chr11p14.1: 29,195,161–31,349,732 and a 10.5-Mb region of chr11p13p12: 32,990,627–43,492,580. As a consequence, 1.6 Mb region of the WAGR syndrome critical region was intact between the two deletions. This patient showed no symptom of WAGR syndrome and no autistic behaviors. Therefore, the region responsible for severe developmental delay and autistic features on WAGR syndrome can be narrowed down to the region remaining intact in Patient 2. Thus, the unique genotype identified in this study suggested that haploinsufficiencies of *PAX6* or *PRRG4* included in this region are candidate genes for severe developmental delay and autistic features characteristic of WAGR syndrome.

Key words: WAGR syndrome; autistic feature; *WT1*; *PAX6*; *PRRG4*

How to Cite this Article:
Yamamoto T, Togawa M, Shimada S, Sangu N, Shimojima K, Okamoto N. 2014. Narrowing of the responsible region for severe developmental delay and autistic behaviors in WAGR syndrome down to 1.6 Mb including *PAX6*, *WT1*, and *PRRG4*. Am J Med Genet Part A 164A:634–638.

INTRODUCTION

Interstitial deletions of the 11p13 region are known to cause WAGR (Wilms tumor, aniridia, genitourinary malformation, and mental retardation) syndrome [Riccardi et al., 1978; Francke et al., 1979; Fischbach et al., 2005]. Subsequent research identified the Wilms tumor 1 gene (*WT1*) and the paired box 6 gene (*PAX6*), located in this narrow 700 kb region, as the genes responsible for Wilms tumor/nephropathies and aniridia, respectively [Call et al., 1990; Gessler et al., 1990; Ton et al., 1991]. Thus, WAGR syndrome is now recognized as a contiguous gene deletion syndrome [Fischbach et al., 2005]. Severe intellectual disability and autistic features are

None of the authors has any conflict of interest to disclose.
Grant sponsor: Ministry of Education, Culture, Sports, Science and Technology (MEXT); Grant sponsor: Ministry of Health, Labor, and Welfare, Japan; Grant sponsor: Japan Society for the Promotion of Science (JSPS).
*Correspondence to:
Toshiyuki Yamamoto, Ph.D., M.D., Tokyo Women's Medical University Institute for Integrated Medical Sciences, 8-1 Kawada-cho, Shinjuku-ward, Tokyo 162-8666, Japan.
E-mail: yamamoto.toshiyuki@twmu.ac.jp
Article first published online in Wiley Online Library (wileyonlinelibrary.com): 19 December 2013
DOI 10.1002/ajmg.a.36325

frequently seen in patients with WAGR syndrome associated with chromosomal deletions of 11p14 regions [Xu et al., 2008]. Thus, it is still controversial which gene within this region is responsible for these neurological manifestations.

Recently, we identified two overlapping deletions of 11p12–p14.1, one of which avoided the involvement of *WT1* and *PAX6*. Indeed, the patient whose deletions allowed both genes to remain intact showed only mild developmental delays and no symptom of WAGR syndrome or autism. Herein, we discuss the genotype–phenotype correlation of this region.

MATERIALS AND METHODS

Materials

Patients' blood samples were obtained under written informed consent based upon approval of the ethical committee of Tokyo Women's Medical University. Genomic DNA was extracted from blood samples using a QIAamp DNA extraction kit (Qiagen, Hilden, Germany) and was used for subsequent evaluation. Metaphase spreads were also prepared from blood samples and used for fluorescence in situ hybridization (FISH) analyses.

Molecular and Cytogenetic Analysis

Genomic copy numbers were analyzed using Agilent Human Genome microarray CGH + SNP180K for Patient 1 and −60 K for Patient 2 (Agilent Technologies, Santa Clara, CA) according to the manufacturer's protocol. To confirm the result of chromosomal microarray testing, FISH analysis was performed using the following human bacterial artificial chromosomes (BACs) as the probes: RP11–358N12 (chr11:31,590,745–31,752,345), RP11–245G17 (chr11: 35,333,079–35,486,953), and RP11–469N6 (chr11:134,478,780–134,651,287) referring build19, which were selected from the UCSC genome browser (http://www.genome.uscs.edu/) (GRCh37/hg19).

RESULTS

Patients' Report

Two patients were determined to have the deletions of 11p14 region.

Patient 1

A 3-year-and-7-month-old boy was born at 38 weeks and 6 days of gestation, with a birth weight of 2,940 g (−0.7 standard deviation [SD]), length of 48 cm (−0.4 SD), and occipito-frontal circumference (OFC) of 34 cm (+0.4 SD). At birth, bilateral congenital cataract, bilateral post-axial polydactyly, and bilateral undescended testes were noted. Then, polydactyly was repaired by plastic surgery and undescended testes were fixed into the scrotum. However, ophthalmological examination revealed bilateral corneal opacity and aniridia, indicated that ophthalmological surgery was impossible. He showed developmental delay with head control at 5 months, rolling over at 8 months, and walking unsupported at 28 months. Brain magnetic resonance imaging showed no abnormalities. Abdominal ultrasonography did not detect the presence of tumors.

At present, he shows severe growth deficiency, with a height of 84 cm (−3.4 SD), weight of 9.5 kg (−3.0 SD), and OFC of 50 cm (−0.8 SD), despite receiving sufficient nutritional support. His facial characteristics are distinctive, with a depressed nasal bridge, bilaterally downslanting palpebral fissures with ptosis, and bilateral low-set ears. Because he can only detect brightness, he attends special day care center. Continuous ophthalmologic examination reveals strabismus, staphyloma on the right eye, and progressive bilateral glaucoma. He showed autistic behaviors including strong tenacity and anxiety, remarkable hypersensitivity for sound and touch, and temper tantrum especially when his routine activities were disturbed. There is still no meaningful word. Psychological testing by Kyoto Scale of Psychological Development 2001 indicates severe developmental delay with a total developmental quotient (DQ) of 23 (postural-motor of 42, cognitive-adaptive of 16, and language-social of 23) [Kanemaru et al., 2013]. Conventional G-banding showed normal male karyotype of 46,XY.

Patient 2

A 2-year-old girl was born at 37 weeks of gestation by cesarean, with a low birth weight of 2,406 g (−1.7 SD), length of 43 cm (−3.1 SD), OFC of 32.5 cm (−0.5 SD). Her older brother had experienced early infantile developmental delay, but has now recovered. Her younger brother showed no abnormalities. The patient had a past history of congenital dislocation of the hip, which was treated with a Pavlik harness. Thus, during the infantile period, she exhibited motor developmental delays with head control at 5 months, sitting at 10 months, and crawling at 12 months, believed to be a consequence of her hip condition. However, at 1 year of age, the patient showed no meaningful speech. Thus, she was referred to our hospital at 16 months of age.

At 16 months of age, she showed severe growth deficiency, with a height of 68.4 cm (−3.5 SD), weight of 9.2 kg (−0.3 SD), and OFC of 46 cm (−0.7 SD). Her distinctive facial features included microretrognathia and low-set ears. She showed shyness, but laughed when she was dandled. Nonverbal communication by eye contact and pointing was good. She could sit alone, but needed support to stand. Neurological examination revealed mild hypotonia. Ophthalmological examination revealed hyperopic astigmatism, but no abnormalities in the cornea, lens, iris, or ocular fundus. Abdominal ultrasonography did not detect the presence of tumors.

At present, she shows short stature, with a height of 75.6 cm (−3.0 SD), weight of 11.9 kg (+0.8 SD), and OFC of 47.4 cm (+0.1 SD). She can run by herself and can communicate by gestures, but still spoke no meaningful words; however, her interpersonal skill is good enough to deny autism spectrum disorders. The Enjoji scale for development indicated mild developmental delay [Numata et al., 2013], with a DQ of 69 with physical abilities of the whole body at 18 months old level; skilled hand motor activities at 18 months; behavior at 14 months; interpersonal skills at 24 months; speech ability at 8 months; and language comprehension at 18 months. Conventional G-banding showed an interstitial deletion of chromosome 11, with karyotype of 46,XX,del(11)(p11.2p13).

Chromosomal Deletions

In Patient 1, chromosomal microarray testing revealed a genomic copy number aberration with a size of 8.6 Mb in chromosome 11, represented as arr 11p14.1p12(29,676,434–38,237,948) × 1 (Fig. 1; Table I), according to build19. FISH analysis confirmed the deletion in this patient (Fig. 2A). In Patient 2, chromosomal microarray testing was performed to determine the deletion region of 11p11.2-p13, which was initially identified by conventional G-banding. The result revealed two regions were deleted, with the sizes of 2.2 and 10.5 Mb in chromosome 11, and the 1.6 Mb region was intact between two deletions, represented as arr 11p14.1(29,195,161–31,349,732) × 1,11p13p12(32,990,627–43,492,580) × 1 (Fig. 1; Table I), according to build19. FISH analysis confirmed the deletion and intact region in this patient (Fig. 2B, C). There was no other pathogenic chromosomal aberration in both patients. Parents of both patients declined to be karyotyped for themselves.

DISCUSSION

In this study, we identified chromosomal deletions involving 11p13 region in two independent patients. Although the total affected region in Patient 1 was smaller than that in Patient 2, clinical features, including developmental delay and autistic behaviors, were more severe in Patient 1 (Fig. 1). This discrepancy could be derived from the intact region identified in Patient 2 (Tables I and II).

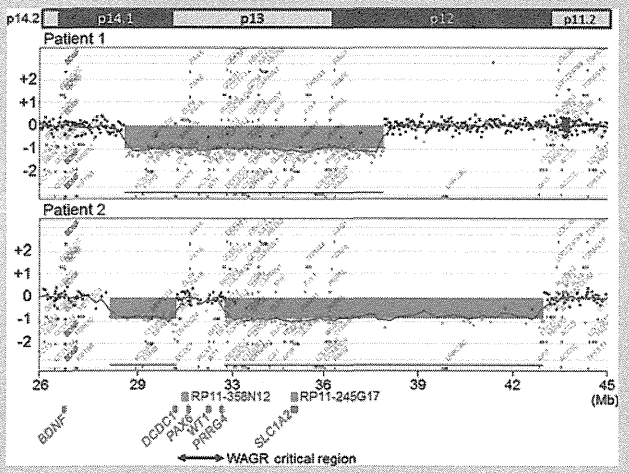

FIG. 1. The results of chromosomal microarray testing and genome maps. The aberration regions seen in the two patients are diagramed using the Chromosome View of Agilent Genomic Workbench (Agilent Technologies). Patient 1 shows loss of genomic copy numbers with a size of 8.6 Mb in chromosome 11. On the other hand, Patient 2 shows two aberration regions with sizes of 2.2 and 10.5 Mb in chromosome 11. *X*- and *Y*-axes indicate genomic positions and $\log_2$ ratios of probe intensities. Aberrant regions are shown by blue translucent rectangles. Green rectangles indicate the locations of the FISH probes used in this study. Red rectangles indicate the locations of the genes discussed in the text. *PAX6*, *WT1*, and *PRRG4* are located in the intact region in Patient 2. (Although CGH + SNP array was used for Patient 1, only CGH panel is shown to compare with Patient 2.)

Patient 1 showed typical features of WAGR syndrome, and this was supported by the fact that the deletion region included *WT1* and *PAX6*. In addition, this patient also showed severe developmental delay and autistic behaviors. Many patients with WAGR syndrome show developmental delays and autistic features that can be derived from the genes included in the deletion region. Thus, neurological phenotypes of the patients depend on the deleted region and the genes involved in the deleted region. Fischbach et al. [2005] reported that about 20% of patients with WAGR syndrome show autistic features. Xu et al. [2008] compared deletion regions identified in patients with WAGR syndrome and analyzed the genes that may contribute to developmental delays and autism. Among 31 patients, 16 (52%) were diagnosed with autism. The solute carrier Family 1 (glial high affinity glutamate transporter) member 2 gene (*SLC1A2*) was included in the deleted region in 22 patients, of whom 13 (59%) were diagnosed with autism. *SLC1A2* encodes one of the glutamate transporters, which are membrane-bound proteins localized in glial cells or presynaptic glutamatergic nerve endings [Xu et al., 2008]. Additionally, the brain-derived neurotrophic factor gene (*BDNF*) was included in the deletion region of 19 patients, of whom 13 (68%) were diagnosed with autism [Xu et al., 2008]. Shinawi et al. [2011] reported four patients showing neurobehavioral abnormalities associated with microdeletions of 11p14.1, which extended distal to the WAGR critical region. Because *BDNF* was included in the SRO among them, *BDNF* may have a significant role in neurobehavioral problems including autism. More recently, haploinsufficiency of *BDNF* was shown to be associated with lower adaptive behavior and reduced cognitive functioning [Han et al., 2013]. Xu et al. [2008] also reported that the other candidate gene, the proline rich Gla (G-carboxyglutamic acid) 4 gene (*PRRG4*), located near *WT1*, was included in the deletions identified in all 31 patients, although little is known for the function of this gene. From these data, Xu et al. [2008] concluded that these three genes, *BDNF*, *SLC1A2*, and *PRRG4*, may contribute to autism.

Davis et al. [2008] identified a 1.3-Mb deletion in the 3′ region of *PAX6* in a patient with aniridia, autism, and intellectual disability. This region can disrupt normal function of *PAX6*, thereby resulting in aniridia [Cheng et al., 2011]. Because this region includes double cortin related genes, that is, the doublecortin domain containing 1 gene (*DCDC1*), Davis et al. [2008] suggested the possibility that this region may contribute to autism. In addition, some reports have suggested an association between *PAX6* mutations and autism/intellectual disability [Heyman et al., 1999; Chao et al., 2003; Dansault et al., 2007]. Thus, it is still unclear which genes cause susceptibility to autism. In this study, *BDNF* was not included in the deletion regions of either patient. Thus, *BDNF* was not the gene responsible for the neurological features of Patient 1, which included severe developmental delay and autistic features.

In this study, Patient 2 showed a milder phenotype, without symptoms of WAGR syndrome or autistic behaviors; however, this patient did have a large chromosomal deletion of 11p, as shown by G-banding. The results of chromosomal microarray testing revealed that the deleted region was split into two regions, and

TABLE I. Summary of Chromosomal Microarray Testing

Cytoband	Probe name	Start[a]	Stop[a]	Patient 1	Patient 2
p14.1	A_16_P19193104	29,062,145	29,062,204	Not Del	Not Del
p14.1	A_14_P138456	29,195,161	29,195,220	NA	Del
p14.1	A_16_P02418841	29,634,061	29,634,120	Not Del	NA
p14.1	A_16_P19194550	29,676,434	29,676,493	Del	NA
p13	A_14_P100247	31,349,673	31,349,732	NA	Del
p13	A_14_P131630	31,391,205	31,391,253	NA	Not Del
p13	A_14_P129993	32,975,692	32,975,751	NA	Not Del
p13	A_14_P104655	32,990,627	32,990,686	NA	Del
p12	A_16_P19215393	38,237,889	38,237,948	Del	NA
p12	A_18_P11065446	38,274,526	38,274,585	Not Del	NA
p12	A_14_P117186	43,492,521	43,492,580	NA	Del
p12	A_14_P113471	43,512,463	43,512,522	NA	Not Del

Not Del, not deleted; NA, probe is not available; DEL, deleted. Gray columns indicate the deletion regions.
[a]The genomic positions are referred to build19.

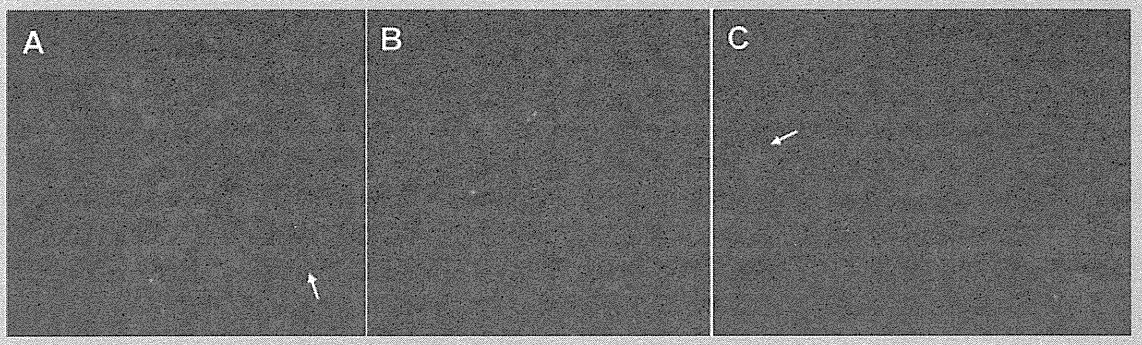

FIG. 2. Results of FISH analyses. Although there is only one signal of RP11–358N12 labeled by the spectrum green in metaphase spread of Patient 1 (A), there are two green signals of RP11–358N12 in that of Patient 2 (B), indicating the deletion of this region only in Patient 1. Only one signal is observed for RP11–245G17 labeled by the spectrum green in the metaphase spread of Patient 2 (C), indicating the deletion of 11p13 in Patient 2. In all metaphase spreads, the two signals labeled for RP11–469N6 by the spectrum orange are the markers for 11q25. Arrows indicate abnormal chromosome 11 having no green signal.

TABLE II. The Genes Around the Intact Region Between Two Deletions Identified in Patient 2

Gene name	Position in chromosome 11[a]
Doublecortin domain containing 1 (*DCDC1*)	30,964,749–31,391,357
DnaJ (Hsp40) homolog, subfamily C, member 24 (*DNAJC24*)	31,391,377–31,454,382
IMP1 inner mitochondrial membrane peptidase-like (*IMMP1L*)	31,453,949–31,531,169
Elongation protein 4 homolog (*ELP4*)	31,531,297–31,805,329
Paired box 6 (*PAX6*)	31,806,340–31,839,509
Reticulocalbin 1, EF-hand calcium binding domain (*RCN1*)	31,838,114–32,127,272
Wilms tumor 1 (*WT1*)	32,409,322–32,457,081
Eukaryotic translation initiation factor 3, subunit M (*EIF3M*)	32,605,391–32,624,014
Coiled-coil domain containing 73 (*CCDC73*)	32,623,626–32,816,187
Proline rich Gla (G-carboxyglutamic acid) 4 (transmembrane) (*PRRG4*)	32,851,481–32,879,669
Glutamine and serine rich 1 (*QSER1*)	32,914,792–33,001,814

Because the minimum region of the proximal deletion ends at chr11:31,349,732 and the minimum region of the centromeric deletion starts at chr11:32,990,627, genes located on both sides of the intact region, *DCDC1* and *QSER1*, are partially included in the deletion regions.
[a]The genomic positions are referred to build19.

the critical region for WAGR syndrome remained intact. This result was in accordance with the lack of phenotypic feature of WAGR syndrome in this patient. Alternatively, *SLC1A2* and *DCDC1* were included in the deleted region of Patient 2, indicating that haploinsufficiencies of these genes do not cause autistic features.

Therefore, from our data, the region responsible for the severe developmental delay and autistic behaviors on WAGR syndrome can be narrowed down to the region remaining intact in Patient 2. Thus, haploinsufficiencies of *PAX6* per se may be considered potential candidates. Furthermore, *PRRG4*, which is also located in this region, may be a candidate gene for the development of autistic features, as shown by the unique genotype identified in this study.

ACKNOWLEDGMENTS

We would like to express our gratitude to the patients and their families for their cooperation. This work was partially supported by a Grant-in-Aid for Scientific Research on Innovative Areas "Foundation of Synapse and Neurocircuit Pathology" from the Ministry of Education, Culture, Sports, Science and Technology (MEXT) (T.Y.); a Grant-in-Aid for Scientific Research from Health Labor Sciences Research Grants from the Ministry of Health, Labor, and Welfare, Japan (T.Y.); and a Grant-in-Aid for Young Scientists (B) from Japan Society for the Promotion of Science (JSPS) (K.S.).

REFERENCES

Call KM, Glaser T, Ito CY, Buckler AJ, Pelletier J, Haber DA, Rose EA, Kral A, Yeger H, Lewis WH, et al. 1990. Isolation and characterization of a zinc finger polypeptide gene at the human chromosome 11 Wilms' tumor locus. Cell 60:509–520.

Chao LY, Mishra R, Strong LC, Saunders GF. 2003. Missense mutations in the DNA-binding region and termination codon in PAX6. Hum Mutat 21:138–145.

Cheng F, Song W, Kang Y, Yu S, Yuan H. 2011. A 556 kb deletion in the downstream region of the PAX6 gene causes familial aniridia and other eye anomalies in a Chinese family. Mol Vis 17:448–455.

Dansault A, David G, Schwartz C, Jaliffa C, Vieira V, de la Houssaye G, Bigot K, Catin F, Tattu L, Chopin C, Halimi P, Roche O, Van Regemorter N, Munier F, Schorderet D, Dufier JL, Marsac C, Ricquier D, Menasche M, Penfornis A, Abitbol M. 2007. Three new PAX6 mutations including one causing an unusual ophthalmic phenotype associated with neurodevelopmental abnormalities. Mol Vis 13:511–523.

Davis LK, Meyer KJ, Rudd DS, Librant AL, Epping EA, Sheffield VC, Wassink TH. 2008. Pax6 3′ deletion results in aniridia, autism and mental retardation. Hum Genet 123:371–378.

Fischbach BV, Trout KL, Lewis J, Luis CA, Sika M. 2005. WAGR syndrome: A clinical review of 54 cases. Pediatrics 116:984–988.

Francke U, Holmes LB, Atkins L, Riccardi VM. 1979. Aniridia-Wilms' tumor association: Evidence for specific deletion of 11p13. Cytogenet Cell Genet 24:185–192.

Gessler M, Poustka A, Cavenee W, Neve RL, Orkin SH, Bruns GA. 1990. Homozygous deletion in Wilms tumours of a zinc-finger gene identified by chromosome jumping. Nature 343:774–778.

Han JC, Thurm A, Golden Williams C, Joseph LA, Zein WM, Brooks BP, Butman JA, Brady SM, Fuhr SR, Hicks MD, Huey AE, Hanish AE, Danley KM, Raygada MJ, Rennert OM, Martinowich K, Sharp SJ, Tsao JW, Swedo SE. 2013. Association of brain-derived neurotrophic factor (BDNF) haploinsufficiency with lower adaptive behaviour and reduced cognitive functioning in WAGR/11p13 deletion syndrome. Cortex (in press). DOI: 10.1016/j.cortex.2013.02.009

Heyman I, Frampton I, van Heyningen V, Hanson I, Teague P, Taylor A, Simonoff E. 1999. Psychiatric disorder and cognitive function in a family with an inherited novel mutation of the developmental control gene PAX6. Psychiatr Genet 9:85–90.

Kanemaru N, Watanabe H, Kihara H, Nakano H, Takaya R, Nakamura T, Nakano J, Taga G, Konishi Y. 2013. Specific characteristics of spontaneous movements in preterm infants at term age are associated with developmental delays at age 3 years. Dev Med Child Neurol 55:713–721.

Numata Y, Onuma A, Kobayashi Y, Sato-Shirai I, Tanaka S, Kobayashi S, Wakusawa K, Inui T, Kure S, Haginoya K. 2013. Brain magnetic resonance imaging and motor and intellectual functioning in 86 patients born at term with spastic diplegia. Dev Med Child Neurol 55:167–172.

Riccardi VM, Sujansky E, Smith AC, Francke U. 1978. Chromosomal imbalance in the Aniridia-Wilms' tumor association: 11p interstitial deletion. Pediatrics 61:604–610.

Shinawi M, Sahoo T, Maranda B, Skinner SA, Skinner C, Chinault C, Zascavage R, Peters SU, Patel A, Stevenson RE, Beaudet AL. 2011. 11p14.1 microdeletions associated with ADHD, autism, developmental delay, and obesity. Am J Med Genet Part A 155A:1272–1280.

Ton CC, Hirvonen H, Miwa H, Weil MM, Monaghan P, Jordan T, van Heyningen V, Hastie ND, Meijers-Heijboer H, Drechsler M, et al. 1991. Positional cloning and characterization of a paired box- and homeobox-containing gene from the aniridia region. Cell 67:1059–1074.

Xu S, Han JC, Morales A, Menzie CM, Williams K, Fan YS. 2008. Characterization of 11p14-p12 deletion in WAGR syndrome by array CGH for identifying genes contributing to mental retardation and autism. Cytogenet Genome Res 122:181–187.

Expanding the phenotypic spectrum of *TUBB4A*-associated hypomyelinating leukoencephalopathies

Satoko Miyatake, MD, PhD
Hitoshi Osaka, MD, PhD
Masaaki Shiina, MD, PhD
Masayuki Sasaki, MD, PhD
Jun-ichi Takanashi, MD, PhD
Kazuhiro Haginoya, MD, PhD
Takahito Wada, MD, PhD
Masafumi Morimoto, MD, PhD
Naoki Ando, MD, PhD
Yoji Ikuta, MD
Mitsuko Nakashima, MD, PhD
Yoshinori Tsurusaki, PhD
Noriko Miyake, MD, PhD
Kazuhiro Ogata, MD, PhD
Naomichi Matsumoto, MD, PhD
Hirotomo Saitsu, MD, PhD

Correspondence to Dr. Matsumoto: naomat@yokohama-cu.ac.jp or Dr. Saitsu: hsaitsu@yokohama-cu.ac.jp

ABSTRACT

Objective: We performed whole-exome sequencing analysis of patients with genetically unsolved hypomyelinating leukoencephalopathies, identifying 8 patients with *TUBB4A* mutations and allowing the phenotypic spectrum of *TUBB4A* mutations to be investigated.

Methods: Fourteen patients with hypomyelinating leukoencephalopathies, 7 clinically diagnosed with hypomyelination with atrophy of the basal ganglia and cerebellum (H-ABC), and 7 with unclassified hypomyelinating leukoencephalopathy, were analyzed by whole-exome sequencing. The effect of the mutations on microtubule assembly was examined by mapping altered amino acids onto 3-dimensional models of the αβ-tubulin heterodimer.

Results: Six heterozygous missense mutations in *TUBB4A*, 5 of which are novel, were identified in 8 patients (6/7 patients with H-ABC [the remaining patient is an atypical case] and 2/7 patients with unclassified hypomyelinating leukoencephalopathy). In 4 cases with parental samples available, the mutations occurred de novo. Analysis of 3-dimensional models revealed that the p.Glu410Lys mutation, identified in patients with unclassified hypomyelinating leukoencephalopathy, directly impairs motor protein and/or microtubule-associated protein interactions with microtubules, whereas the other mutations affect longitudinal interactions for maintaining αβ-tubulin structure, suggesting different mechanisms in tubulin function impairment. In patients with the p.Glu410Lys mutation, basal ganglia atrophy was unobserved or minimal although extrapyramidal features were detected, suggesting its functional impairment.

Conclusions: *TUBB4A* mutations cause typical H-ABC. Furthermore, *TUBB4A* mutations associate cases of unclassified hypomyelinating leukoencephalopathies with morphologically retained but functionally impaired basal ganglia, suggesting that *TUBB4A*-related hypomyelinating leukoencephalopathies encompass a broader clinical spectrum than previously expected. Extrapyramidal findings may be a key for consideration of *TUBB4A* mutations in hypomyelinating leukoencephalopathies. ***Neurology*® 2014;82:2230–2237**

GLOSSARY

4H = hypomyelination, hypodontia, and hypogonadotropic hypogonadism; **H-ABC** = hypomyelination with atrophy of the basal ganglia and cerebellum; **MAP** = microtubule-associated protein; **MREI** = Met-Arg-Glu-Ile; ***TUBB4A*** = tubulin, beta 4A class IVa.

Leukoencephalopathies are a heterogeneous group of disorders affecting the white matter of the brain. It is estimated that approximately 30% to 40% of patients with leukoencephalopathy remain without a specific diagnosis despite extensive investigations.[1] Brain MRI aids diagnosis because distinct MRI patterns enable easier detection of white matter abnormalities and successful categorization.[1,2] Moreover, recent advances in whole-exome sequencing have improved understanding of these clinically defined/undefined disease entities by identifying genetic causes and their phenotypic spectrum. For example, the majority of cases with hypomyelination,

Supplemental data at Neurology.org

From the Departments of Human Genetics (S.M., M.N., Y.T., N. Miyake, N. Matsumoto, H.S.) and Biochemistry (M. Shiina, K.O.), Yokohama City University Graduate School of Medicine; Division of Neurology (H.O.), Clinical Research Institute, Kanagawa Children's Medical Center, Yokohama; Department of Pediatrics (H.O.), Jichi Medical School, Tochigi; Department of Child Neurology (M. Sasaki), National Center of Neurology and Psychiatry, Tokyo; Department of Pediatrics (J.-i.T.), Kameda Medical Center, Chiba; Department of Pediatric Neurology (K.H.), Takuto Rehabilitation Center for Children, Sendai; Genetic Counselling and Clinical Research Unit (T.W.), Kyoto University School of Public Health; Department of Pediatrics (M.M.), Graduate School of Medical Science, Kyoto Prefectural University of Medicine; Department of Neonatology and Pediatrics (N.A.), Nagoya City University Graduate School of Medical Sciences; and Department of Neurology (Y.I.), Tokyo Metropolitan Children's Medical Center, Japan.

Go to Neurology.org for full disclosures. Funding information and disclosures deemed relevant by the authors, if any, are provided at the end of the article.

hypodontia, and hypogonadotropic hypogonadism (4H syndrome),[3–5] tremor-ataxia with central hypomyelination leukodystrophy (TACH),[6] leukodystrophy with oligodontia (LO),[7,8] or hypomyelination with cerebellar atrophy and hypoplasia of the corpus callosum (HCAHC),[9] which was described in Japan, share some clinical overlap and have *POLR3A* or *POLR3B* mutations in common.[10–14]

Hypomyelination with atrophy of the basal ganglia and cerebellum (H-ABC)[15,16] is characterized by early-onset motor regression and/or delay followed by extrapyramidal symptoms, distinguishing H-ABC from other hypomyelinating leukoencephalopathies caused by *POLR3A* or *POLR3B* mutations. A recurrent de novo *TUBB4A* mutation was recently reported in 11 patients with H-ABC.[17] Of note, *TUBB4A* mutations also cause autosomal dominant DYT4 dystonia,[18,19] a condition that presents with normal brain MRI findings. This suggests that in addition to H-ABC, *TUBB4A* mutations may be widely related to other hypomyelinating leukoencephalopathies. Herein, we describe 8 patients with *TUBB4A* mutations identified by whole-exome sequencing, clarifying their phenotypic spectrum.

METHODS Study subjects. Fourteen patients with molecularly undiagnosed hypomyelinating leukoencephalopathy were included in the study. Patients were diagnosed based on clinical symptoms and brain MRI findings. Among the 14 patients, 7 were clinically diagnosed with H-ABC and 7 with hypomyelinating leukoencephalopathy that did not meet the criteria for H-ABC, 4H syndrome, or Pelizaeus-Merzbacher disease. Patients with *POLR3A* or *POLR3B* mutations were excluded from this cohort. When available, parental samples were also tested in mutation-positive patients.

Standard protocol approvals, registrations, and patient consents. Experimental protocols were approved by the Committee for Ethical Issues at Yokohama City University School of Medicine. Written informed consent was obtained from all patients or their parents.

Mutation analysis. We performed whole-exome sequencing in 14 patients. Genomic DNA was captured using the SureSelect^{XT} Human All Exon 50 Mb (v3) or 51 Mb (v4) Kit (Agilent Technologies, Santa Clara, CA) and sequenced on either the GAIIx platform (Illumina, San Diego, CA) with 108–base pair paired-end reads or HiSeq2000 (Illumina) with 101–base pair paired-end reads. After filtering against dbSNP135 and 91 in-house normal control exomes, rare protein-altering and splice-site variant calls were obtained for each patient. We identified *TUBB4A* mutation calls and confirmed these mutations by Sanger sequencing. In 4 of 8 patients with *TUBB4A* mutations, parental samples were analyzed by Sanger sequencing to determine the mode of inheritance.

Three-dimensional structure modeling. To determine the effect of *TUBB4A* mutations on microtubule assembly, we mapped mutation positions onto the 3-dimensional structure of the αβ-tubulin heterodimer (Protein Data Bank code 1JFF)[20] and examined their interaction with surrounding molecules.

RESULTS Identification of *TUBB4A* mutations. Whole-exome sequencing identified 6 heterozygous missense mutations in *TUBB4A*, in 6 of 7 patients with H-ABC (85.7%) and 2 of 7 patients with unclassified hypomyelinating leukoencephalopathy (28.6%) (see table 1 and tables e-1 and e-2 on the *Neurology*® Web site at Neurology.org). Two mutations, c.1228G>A (p.Glu410Lys) and c.745G>A (p.Asp249Asn), were identified in 2 unrelated patients. Two hypomyelinating patients with similar clinical features as those previously reported,[9] carried the c.1228G>A mutation. The c.745G>A mutation was a recurrent mutation reported in patients with H-ABC.[17] The other 5 mutations were novel. None of the mutations were registered in the National Heart, Lung, and Blood Institute Exome Sequencing Project (ESP6500), 1000 Genomes, or our 575 in-house control exomes. The c.5G>A (p.Arg2Gln) missense mutation, identified in a patient with H-ABC, alters Arg2 to Gln. Arg2 is located within the highly conserved, amino-terminal β-tubulin tetrapeptide Met-Arg-Glu-Ile (MREI) motif and is involved in autoregulatory mechanisms for β-tubulin stability. Notably, Arg2 is altered to Gly in a large family with DYT4.[18,19] All of the mutations occur within highly conserved residues, from yeast to human, and among human β-tubulins (figure 1). GERP (Genomic Evolutionary Rate Profiling) scores were high for all mutated residues, and Web-based prediction programs identified all mutations as pathogenic (table e-1). In 4 patients with parental samples available, the mutations occurred de novo (table e-1). In 2 patients, only the mother's sample was available and confirmed as mutation-negative.

Three-dimensional structural modeling analysis. Tubulin heterodimers polymerize longitudinally in a head-to-tail manner, forming protofilaments, which then laterally interact with each other to form microtubules (figure 2). Some mutations fall within longitudinal interaction interfaces, whereas others are near interaction regions for motor proteins and microtubule-associated proteins (MAPs).[21,22] Thr178 of β-tubulin is located at a longitudinal interheterodimer interface, in proximity to the guanine nucleotide–binding pocket of β-tubulin (figure 2). This residue is reportedly important for regulation of αβ-tubulin heterodimer polymerization with GTP[23,24]; therefore, the Thr178Arg mutation may affect the polymerization process. Arg2 and Asp249 of β-tubulin are

Table 1 Clinical features of the patients

	Patient 1[9]	Patient 2[9]	Patient 3	Patient 4[26]	Patient 5[27]	Patient 6	Patient 7	Patient 8
Current age, y, sex	23, M	41, M	15, F	12, M	16, M	10, M	4, M	1, F
Mutation	c.1228G>A	c.1228G>A	c.5G>A	c.745G>A	c.1162A>G	c.745G>A	c.533C>G	c.785G>A
Protein alteration	p.Glu410Lys	p.Glu410Lys	p.Arg2Gln	p.Asp249Asn	p.Met388Val	p.Asp249Asn	p.Thr178Arg	p.Arg262His
Initial diagnosis	Unclassified hypomyelinating leukoencephalopathy[a]	Unclassified hypomyelinating leukoencephalopathy[a]	H-ABC	H-ABC	H-ABC	H-ABC	H-ABC	H-ABC
Age at onset, mo	12	12	1.5	18	3	19	6	2
Maximum motor milestone	Unsupported unstable walking	Unsupported unstable walking	No head control	Walking for a few steps	Rolling over	Supported walking	No head control	No head control
Onset of motor deterioration	10 y	20 y	ND	18 mo	3 mo	19 mo	ND	ND
Intellectual disability	Mild	Moderate	Severe	Severe	Severe	Severe	Severe	Moderate
Motor signs								
Ataxia	+	+	ND	+	ND	+	ND	ND
Tremor	+	+	−	−	−	+	−	ND
Spasticity	+	+	+	+	+	+	ND	+
Babinski sign	+	+	−	+	ND	+	−	+
Rigidity	+	+	+	+	+	+	+	−
Choreoathetosis	−	−	+	+	+	−	−	−
Dystonia	+	+	+	+	+	+	−	−
Brain MRI findings								
Hypomyelination	+	+	+	+	+	+	+	+
Atrophy of the basal ganglia	−	±	+	+	+	+	+	+
Atrophy of the cerebellum	+	+	+	+	+	+	+	−
Atrophy of the corpus callosum	+	+	+	+	+	+	+	−

Abbreviations: H-ABC = hypomyelination with atrophy of the basal ganglia and cerebellum; ND = not determined.
Symbols: + = present; − = absent; ± = minimally detected.
[a] Unclassified hypomyelinating leukoencephalopathy: did not meet the criteria for H-ABC, 4H syndrome (hypomyelination, hypodontia, and hypogonadotropic hypogonadism), or Pelizaeus-Merzbacher disease.

located at an intraheterodimer interface (figures 2 and e-1A). These residues stabilize the β-tubulin T7 loop region, which interacts with α-tubulin within a heterodimer (figure e-1A), indicating that the p.Arg2Gln and p.Asp249Asn mutations may affect tubulin heterodimerization. Glu410 is located on the exposed outer surface that mediates interactions with motor proteins and/or MAPs (figures 2 and e-1B).[21,22] This residue is crucial for the kinesin-microtubule interaction, and thus the p.Glu410Lys mutation may directly impair motor protein and/or MAP interactions with microtubules. Arg262 and Met388 are located near the intra- and interheterodimer interfaces, respectively, and both are also near the interaction region for motor proteins and/or MAPs (figures 2 and e-1, B and C). Arg262 is involved in the hydrophobic core with residues from a loop that interacts with the α-tubulin subunit within the heterodimer, and from helix H12, which interacts with motor proteins and/or MAPs (figures 2 and e-1B). Met388 is involved in the hydrophobic core with residues from helix H11, which interacts with the α-tubulin subunit in the neighboring heterodimer, and from helix H12 (figures 2 and e-1C).[25] Thus, the p.Arg262His and the p.Met388Val mutations may destabilize the hydrophobic core and potentially affect the tertiary structure, resulting in impairment of longitudinal intra- and interheterodimer tubulin interactions, respectively, and/or interaction with motor proteins and/or MAPs.

Clinical features. Clinical information on patients with *TUBB4A* mutations is presented in tables 1 and e-2, and brain MRIs are shown in figures 3 and e-2.

The mean age at onset was 9.2 months, although the age at onset was varied. Initial motor development also varied, with some acquiring unsupported but

Figure 1 *TUBB4A* mutations in patients with hypomyelinating leukoencephalopathy

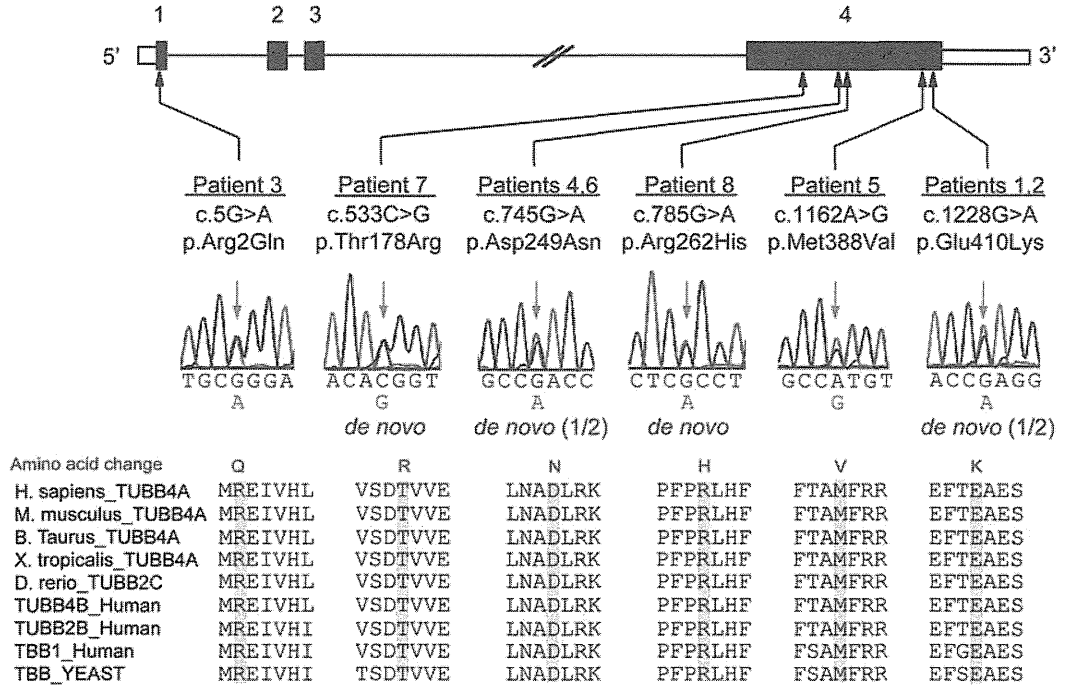

Amino acid change	Q	R	N	H	V	K
H. sapiens_TUBB4A	MREIVHL	VSDTVVE	LNADLRK	PFPRLHF	FTAMFRR	EFTEAES
M. musculus_TUBB4A	MREIVHL	VSDTVVE	LNADLRK	PFPRLHF	FTAMFRR	EFTEAES
B. Taurus_TUBB4A	MREIVHL	VSDTVVE	LNADLRK	PFPRLHF	FTAMFRR	EFTEAES
X. tropicalis_TUBB4A	MREIVHL	VSDTVVE	LNADLRK	PFPRLHF	FTAMFRR	EFTEAES
D. rerio_TUBB2C	MREIVHL	VSDTVVE	LNADLRK	PFPRLHF	FTAMFRR	EFTEAES
TUBB4B_Human	MREIVHL	VSDTVVE	LNADLRK	PFPRLHF	FTAMFRR	EFTEAES
TUBB2B_Human	MREIVHI	VSDTVVE	LNADLRK	PFPRLHF	FTAMFRR	EFTEAES
TBB1_Human	MREIVHI	VSDTVVE	LNADLRK	PFPRLHF	FSAMFRR	EFGEAES
TBB_YEAST	MREIVHI	TSDTVVE	LNADLRK	PFPRLHF	FSAMFRR	EFSEAES

TUBB4A schematic with the 6 mutations is presented. Untranslated regions and coding regions are shown in white and black rectangles, respectively. All mutations occur at evolutionarily conserved amino acids. Homologous sequences were aligned using CLUSTALW (http://www.genome.jp/tools/clustalw/).

unsteady walking and others never acquiring head control. The maximum motor milestone of these patients was unstable short walking. The clinical course appeared milder in patients with an older age at onset. This tendency was most prominent in patients initially diagnosed with unclassified hypomyelinating leukoencephalopathy. For example, the onset of motor deterioration started in the first or second decades in these patients but was between 0 and 3 years old in patients with typical H-ABC. Intellectual disability was mild to moderate in the former but mostly severe in the latter patients.

All clinically evaluated patients with *TUBB4A* mutations demonstrated cerebellar ataxia and spasticity. Except for patient 8, all demonstrated extrapyramidal features such as rigidity, dystonia, or choreoathetosis. In patient 1, dystonia was prominent compared with other hypomyelination patients with either *POLR3A* or *POLR3B* mutations.[9,11] Patient 8 was 1 year old at the time of the study, and brain MRI showed a relatively small but still well-retained putamen compared with healthy subjects of the same age, suggesting that extrapyramidal features may not yet have developed but would likely express as the basal ganglia atrophy progressed. Notably, both hypomyelinating patients with either very mild basal ganglia atrophy (patient 2) or none identifiable (patient 1) demonstrated extrapyramidal signs, suggesting that the basal ganglia may be impaired functionally in these patients as well as other patients with typical H-ABC. Case reports are available in appendix e-1. Patients 1 and 2,[9] 4,[26] and 5[27] were previously described. Retrospectively, patient 2 might be diagnosed with atypical H-ABC because minimal basal ganglia atrophy cannot be excluded. In the patient with H-ABC with no *TUBB4A* mutation, the atrophy of basal ganglia was very mild compared with that of patients with typical H-ABC. However, clinical symptoms are very severe with neither head control nor sitting at 12 years, suggesting that the patient has atypical H-ABC.

DISCUSSION The β- and α-tubulins are major components of microtubules. Microtubules have essential roles in many cellular processes including mitosis, intracellular transport, asymmetric neuronal morphology, and ciliary and flagellar motility.[28] Multiple β-tubulin isotypes are present, with high homology (differing primarily at 15–20 amino acids within the C terminus), and expressed differentially in a tissue-dependent manner.[29] Certain isotypes, namely, β-tubulin isotypes 2A, 2B, 3, and 4A, are neuron-specific proteins and highly expressed in brain.[28] In the nervous system, microtubules provide structure, generate force necessary for neuronal migration, and serve as scaffolds for motor proteins and/or MAPs to transport cargo.[30] In addition to *TUBB4A*-associated leukoencephalopathies[17] and dystonia,[18,19] *TUBA1A*, *TUBB2B*, and *TUBB3*